Received: 2 February 2018 | Accepted: 9 July 2018

DOI: 10.1111/jace.15948

ORIGINAL ARTICLE

Journal of the American Ceramic Society

Biosilicate® scaffolds produced by 3D-printing and direct foaming using preceramic polymers

Hamada Elsayed[1,2] | **Pietro Rebesan**[1] | **Murilo C. Crovace**[3] | **Edgar D. Zanotto**[3] | **Paolo Colombo**[1,4] | **Enrico Bernardo**[1]

[1]Dipartimento di Ingegneria Industriale, University of Padova, Padova, Italy

[2]Ceramics Department, National Research Centre, Cairo, Egypt

[3]Vitreous Materials Laboratory, Department of Materials Engineering, Center for Research, Education and Technology in Vitreous Materials (CeRTEV), Federal University of São Carlos (UFSCar), São Carlos, São Paulo, Brazil

[4]Department of Materials Science and Engineering, The Pennsylvania State University, University Park, Pennsylvania, USA

Correspondence: Enrico Bernardo, Dipartimento di Ingegneria Industriale, University of Padova, Via Marzolo, 9-35131 Padova, Italy (enrico.bernardo@unipd.it).

Funding information
São Paulo Research Foundation—Fapesp CEPID, Grant/Award Number: 2013/0079

Abstract

Monolithic and powdered Biosilicate®, produced by conventional glass-ceramic technology, have been widely recognized as excellent materials for bone tissue engineering applications. In the current research, we focus on an alternative processing route for this material, consisting of the thermal treatment of silicone polymers containing micro-sized oxide fillers, which offers a unique integration between materials synthesis and shaping. In particular, the new method allows obtaining highly porous Biosilicate® glass-ceramics, in the form of 3D printed scaffolds and foams. 3D scaffolds were successfully fabricated by direct writing using an ink based on a silicone polymer and active inorganic fillers, followed by firing in air at 1000°C. The products showed regular geometries, large open porosity (~60 vol%) and still high compressive strength (~7 MPa). Open-cellular foams with porosity up to ~80 vol% were also prepared from liquid silicones mixed with several fillers, including hydrated sodium phosphate. This specific filler acted both as a foaming agent, because of the gas release by dehydration occurring at low temperature, and as a provider of liquid phase upon firing in air, again at 1000°C.

KEYWORDS

additive manufacturing, bioactive glass, Biosilicate® glass-ceramic, polymer-derived-ceramics

1 | INTRODUCTION

Bioactive materials have revolutionized the field of biomedical engineering because of their relevant, versatile features. A great step forward came out with the findings of L.L. Hench, who invented bioactive glasses and paved the way to the so-called third-generation biomaterials, which stimulate a beneficial response from the body, bonding to living tissues (specially bone) and undergoing progressive dissolution.[1] In particular, Hench developed Bioglass® 45S5, a degradable glass with composition $24.5Na_2O–24.5CaO–45.0SiO_2–6.0P_2O_5$ (wt. %), with high calcium content and with a composition close to a ternary eutectic of the $Na_2O–CaO–SiO_2$ diagram.[2] The main discovery was that Bioglass® 45S5 formed such a strong bond with bone that, when subjected to a critical stress, the fracture occurred in the bulk glass and not at the bone/glass interface.[3] This feature remains a distinctive characteristic of 45S5, although many other materials may represent valid alternatives. These materials include bioglasses with different compositions, glass-ceramics, and Ca phosphate-based ceramics.[4,5] A common sign of bioactivity is the formation of a hydroxyl carbonated apatite layer (HCA) on the surface, similar to the mineral fraction of natural bone, when the material is in contact with simulated body fluid (SBF) or it is implanted in the body.[6–8]

In the mid-1990s, numerous efforts combined two of the key features for prosthetic materials, that is, the high

bioactivity, shown by 45S5, and the good mechanical properties (i.e., strength, toughness, and hardness), exhibited by glass-ceramics. This led to a substantial revision of the formulations, also considering the negative impact of crystallization in bioglasses occurring when heat-treated at relatively high temperatures. Specifically, Li et al.[9] demonstrated that the in vitro formation rate of a hydroxycarbonate apatite layer (HCA) on the surface of a 45S5 bioactive glass significantly decreased with the increase in the crystallized volume fraction. In other words, it was suggested that the apatite formation on the glass-ceramic surface could be related to the amount residual glass phase and that it could entirely inhibit by the increase in crystallized volume fraction. Additional investigations, however, clarified that the crystallization of Bioglass 45S5 just delayed, but did not prevent, the HCA formation even in the case of full crystallization.[10,11]

Biosilicate® glass-ceramics were specifically conceived to overcome the delay in HCA formation for a nearly fully crystallized material. The starting glass formulation is close to that of the 45S5 glass, being 23.75Na_2O, 23.75CaO, 48.5SiO_2, and 4.0P_2O_5 (wt.%). Under controlled double-stage heat treatments, this glass undergoes internal crystallization with the formation of one (1P) or two crystalline phases (2P). More precisely, the main crystal phase is a sodium-calcium silicate ($Na_2CaSi_2O_6$), which is present alone or mixed with sodium-calcium phosphate ($NaCaPO_4$). Several in vitro bioactivity tests have shown that the crystallization of the Biosilicate®, whether in solid or scaffold form, does not significantly affect the formation of HCA.[12] The osteoconductivity, osteoinductivity, biocompatibility, and antibacterial properties exhibited by Biosilicate® glass-ceramics are comparable to those of the "golden standard" amorphous 45S5. In addition, Biosilicate® glass-ceramics have important manufacturing features, such as easy machinability and workability, ensuring the ability to obtain different complex geometries. Biosilicate® glass-ceramics have been successfully tested in a number of in vitro, in vivo, and clinical studies for a wide range of tissue engineering applications.[13]

At present, the commercial use of bioactive glasses is mainly restricted to melt-derived components, in the form of powders, granules or small monoliths. Complex cellular shapes may be obtained by viscous flow sintering of fine glass powders, typically by replication of polyurethane foam sacrificial templates, for the manufacturing of open-celled foams, or by direct ink writing of glass/sacrificial binder pastes, for the manufacturing of three-dimensional reticulated scaffolds.[14] Noncrystallized porous scaffolds (foams) may be obtained by a different strategy, that is, using the sol-gel technique, but they have not yet been approved for clinical use.[15] Furthermore, sol-gel techniques are difficult to scale-up in the industry for several reasons, such as the high cost of the raw materials, the use of large amounts of flammable solvents, the associated drying problems, the complexity and the very long duration of the process.[16,17]

The present investigation was aimed at exploring the fabrication of Biosilicate® glass-ceramics from an alternative route, consisting of the thermal treatment of preceramic polymers, in the form of silicone resins, containing micro- and nano-sized fillers. Silica, resulting from the thermo-oxidative decomposition of silicones, easily reacts with the oxides provided by the fillers (consisting of carbonates, hydroxides or oxides). Several bioactive crystalline Ca-based silicate ceramics, according to this process, have been produced and belong to the vast range of "polymer-derived ceramics" (PDC), known for their distinctive shaping possibilities, through direct foaming, extrusion, and additive manufacturing, available before heat treatment (in the polymer state).[18–20]

Interestingly, the PDC approach may be extended to glasses and glass-ceramics. As an example, Ohl et al[21] introduced borax (sodium borate) in a silicone matrix, also embedding Duran® glass powders; the interaction between polymer-derived silica and borax was intended to form a glass with a chemical composition approaching that of the commercial boro-silicate glass used as main filler. Concerning "polymer-derived glass-ceramics", borates and phopshates are useful in offering liquid phase, which first promotes the synthesis of silicate phases (catalyzing the ionic interdiffusion), then transforms into a glass phase upon cooling.[22,23] Despite the unconventional processing, the definition of "glass-ceramics" for these materials remains appropriate, owing to the strong similarity in the phase assemblage with products from the crystallization of glasses with identical overall chemical formulation, as shown in Figure 1.[22,23]

Silicone/fillers mixtures and glasses can be even mixed, with no change in the phase assemblage after firing: in other words, the "PDC route" to glass-ceramics is both alternative and integrative, compared to conventional glass-ceramic technology.[22,24] In this paper, we specifically show that the application of this processing route to the Biosilicate® glass-ceramic paves the way to a new generation of foams, by direct foaming, according to an appropriate choice of fillers, and 3D-printed scaffolds, from direct ink writing, according to a particularly simple process.

2 | EXPERIMENTAL PROCEDURE

2.1 | Starting materials

Two silicone resins, MK (methyl-siloxane, solid) and H62C (methyl-phenyl-siloxane, liquid), were used as silica precursors. These commercial polymers (both from

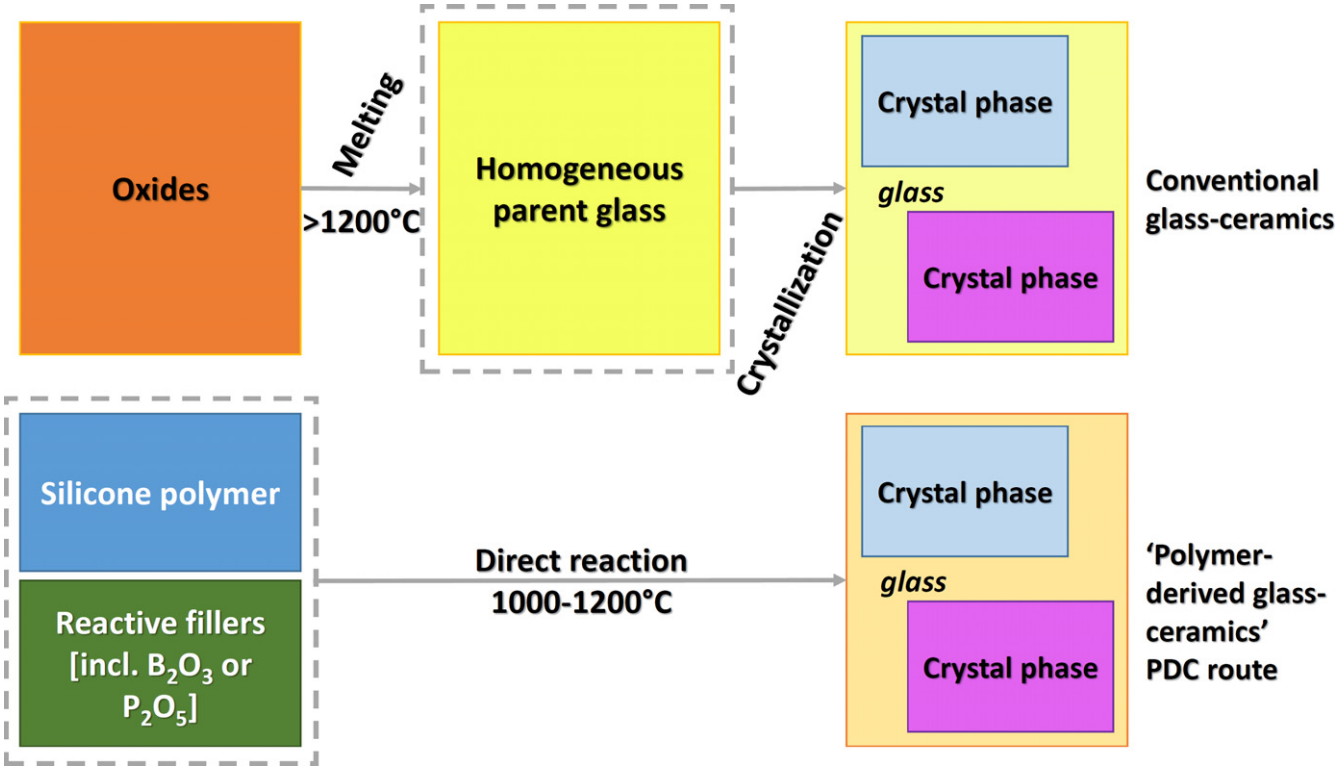

FIGURE 1 Scheme of the process for the development of glass–ceramics via PDC route, compared with conventional glass-ceramic processing [Color figure can be viewed at wileyonlinelibrary.com]

Wacker-Chemie GmbH, Munich, Germany) featured a ceramic yield of 84 wt.% (MK) and 58 wt.% (H62C) after firing in air at 1000°C. Calcium carbonate ($CaCO_3$, <10 μm, Industries Bitossi, Vinci, Italy), sodium carbonate (Na_2CO_3, <38 μm; Sigma-Aldrich Chemie GmbH, Munich, Germany) and anhydrous sodium phosphate dibasic (Na_2HPO_4, <38 μm; Sigma-Aldrich) were used as active fillers. Finally, Biosilicate® glass powder (<5 μm) was added as an inert filler.

2.2 | Preparation of pellets

Biosilicate®, with a composition of 23.75Na_2O, 23.75CaO, 48.5SiO_2, and 4P_2O_5 (wt.%), was melted at 1450°C/3 h in a Pt crucible and poured into water. The glass frit obtained was then subjected to a double-stage heat treatment: first at 565°C/100 h (nucleation) and then at 665°C/1 h (crystal growth). After cooling, the glass-ceramic frit was milled in a disc mill (MA 700—Marconi) and subsequently in a jet mill (CGS 10 Condux—Netzsch). The resulting Biosilicate® powder (average particle size ~5 μm) was used as reference material (G100 formulation, see Table 1).

To make a close comparison with the crystalline phases found in Biosilicate® when developed by the conventional route, careful preparation of the silicone-fillers mixtures had to be carried out, with a precise calculation of the amounts of preceramic polymer and active fillers involved.

MK was dissolved in isopropanol (10 mL for 10 g of final ceramic), and then mixed with $CaCO_3$, Na_2CO_3, and Na_2HPO_4 micro-sized fillers. To ensure the homogeneity, the mixture was kept under magnetic stirring for 15 minutes, and then sonicated for other 15 minutes. Sonication was aimed to eliminate any dissolved gas and disrupt any aggregates formed during the mixing process. The mixtures were poured into large PTFE containers and dried at 80°C overnight.

A glass-ceramic-free formulation consisting of MK polymer and fillers ($CaCO_3$, Na_2CO_3, and Na_2HPO_4) (see formulation G0, in Table 1) was first used to obtain Biosilicate® glass-ceramics after ceramization. This formulation was labeled 100% PDC (PDC = polymer-derived ceramic) since the final material derived from the thermochemical conversion of silicones. Additional formulations were prepared by including Biosilicate® glass powders as further component (formulations G30 and G70); the amounts of silicones and carbonate or phosphate fillers were adjusted to achieve Biosilicate® glass-ceramics composition by integration of the glass with the ceramic material deriving from the silicone/filler reaction.

After drying, the silicone-based mixtures were in the form of solid fragments, which were later converted into fine powders by ball milling at 300 rpm for 30 minutes. Monolithic pellets were prepared using silicone-mixed fillers powders. The powders were cold-pressed in a

TABLE 1 Typical batches for the preparation of glass-ceramic pellets and foams

			Batch formulation						
Label	**Formulation (wt%)**	**Shape**	**MK**	**H62C**	**FS**	**$CaCO_3$**	**Na_2CO_3**	**Na_2HPO_4[a]**	**Biosilicate®**
G100	100% Biosilicate®	Pellet	-	-	-	-	-	-	100
G70	30% PDC-70% Biosilicate®	Pellet	40.52	-	-	29.74	24.36	5.39	70
G30	70% PDC-30% Biosilicate®	Pellet	40.56	-	-	29.82	24.30	5.32	30
G0	100% PDC	Pellet	40.58	-	-	29.82	24.33	5.27	-
		Foam	40.58	-	-	29.82	24.33	5.27[a]	-
G0B	90% PDC-10% Biosilicate®	Foam	40.56	-	-	29.82	24.30	5.32[a]	30
G0L	100% PDC	Foam	-	49.67	-	25.25	20.61	4.47 [a]	-
G0S	100% PDC	Scaffold	36.73	-	3.47	30.01	24.49	5.31	-

[a]Filler in hydrated form ($HNa_2PO_4{\cdot}7H_2O$).

cylindrical steel die (at 40 MPa, for 1 minutes), without any additive, to obtain monolithic pellets (specimens of 1 g, with a diameter of 16.6 mm and a thickness of approximately 3 mm).

2.3 | Direct ink writing of 3D scaffolds

To obtain an ink suitable for 3D printing experiments (starting from G0 formulation) MK silicone was first dissolved in 27.5 vol.% of isopropanol alcohol (C_3H_8O, 2-Propanol, HPLC BASIC, Scharlau, Scharlab Italia srl, Riozzo di Cerro al Lambro [MI], Italy) and then mixed with nano-sized fumed silica (FS; SiO_2, Aerosil R106; Evonik, Essen Germany), average primary particle size was 7 nm, and BET surface area was 220-280 m^2/g (specified by the supplier). The introduction of fumed silica was intended to modify the rheological properties, particularly to provide a pseudoplastic behavior with yield stress, suitable for the printing of suspended struts.[25] According to previous experiences,[26] fumed silica had an optimum impact, as a rheology modifier, by partially replacing the silicone resin as silica source, for an amount of 10 wt.% of the total silica content. Silicone/fumed silica/$CaCO_3$, Na_2CO_3/Na_2HPO_4 proportions were adjusted to keep the overall oxide formulation constant, compared with previous batches. The mixing was performed in an alumina jar, using a planetary ball mill (Pulverisette; Fritsch, Idar-Oberstein, Germany) for 60 minutes at 150 rpm. The mixing process led to a silicone-fumed silica gel, without any agglomerate. Once a clear gel solution was obtained, the other fillers ($CaCO_3$, Na_2CO_3, and Na_2HPO_4) required synthesizing Biosilicate® glass-ceramic were added, according to the weight balances in Table 1.

The ink was transferred into a plastic syringe, which served as a cartridge for direct ink writing. Paste filaments were deposited using a Delta printer (Delta Wasp 2040 Turbo; Waspro-ject, Massa Lombarda, Italy), equipped with a pressurized vessel and an infinite screw for paste extrusion, through a conical nozzle (Nordson EFD, Westlake, OH, USA). Operating with a nozzle diameter of 0.81 mm, 3D scaffolds were fabricated by overlapping extruded filaments from layer-to-layer at 600 μm, along with the z-axis. After printing, the scaffolds were placed overnight in a muffle oven at 80°C in air for drying, to ensure complete evaporation of isopropyl alcohol. All the samples were fired using a heating rate of 1°/min, with holding stages at 500°C, for 3 hours and 1000°C, for 1 hour. The fired samples were then cooled inside the furnace at a rate of 5°C/min.

2.4 | Direct foaming of liquid silicones

MK and H62C polymers were also used as silica precursors for fabricating open-celled foams. H62C was first dissolved in isopropanol (10 mL for 10 g of final ceramic) and then mixed with micro-sized active fillers (see Table 1), achieving stable and homogeneous dispersions. The mixture, after drying overnight at 60°C, turned into a thick paste that was manually transferred into handmade cylindrical Al molds and then subjected to foaming by heating at 350°C in air for 30 minutes. The foaming was formed due to the dehydration of $HNa_2PO_4{\cdot}7H_2O$ filler.[24]

A slightly different procedure was followed for producing foams using solid MK polymer. The silicone was first dissolved in isopropyl alcohol (31.2 vol%), inside a glass beaker and then $CaCO_3$, Na_2CO_3, and $HNa_2PO_4{\cdot}7H_2O$ powders were added. The fillers were incorporated using a mechanical mixer (Argo Lab AM20-D, Carpi, Italy), operating at 900 rpm for 30 minutes. The intensive mixing promoted the homogenization and the progressive evaporation of most of the solvent. The MK-fillers paste was then processed similarly to the H62C-based mixture (casting in Al molds and foaming at 350°C). Both H62C- and MK-based foams were fired according to the same schedule adopted for the 3D scaffolds.

2.5 | Physical and mechanical characterization

DTA/TG analysis (DTA/TGA, STA409; Netzsch Gerätebau GmbH, Selb, Germany) was applied on selected mixtures to assess the transformations associated with the polymer-to-ceramic conversion, decomposition of fillers powders, reaction between silicone and the filler powders as well as the crystallization.

The dimensions of all samples, before and after the heat treatments, were measured using a digital caliper. For dense samples, density determinations were conducted according to the ASTM-C 373 standard.[27] For highly porous samples (of 3D printed and foamed scaffolds), the geometrical density was determined by weighing using a digital balance and computing mass/volume ratios. The apparent and true densities were determined using a helium pycnometer (Micromeritics AccuPyc 1330, Norcross, GA, USA).

Morphological and microstructural characterizations on fired cellular materials were performed using optical stereomicroscopy (AxioCam ERc 5s Microscope Camera; Carl Zeiss Microscopy, Thornwood, NY, USA) and scanning electron microscopy (FEI Quanta 200 ESEM, Eindhoven, The Netherlands) equipped with energy dispersive spectroscopy (EDS). The identification of crystal phases was performed, on powdered samples of the same weight, by X-ray diffraction (XRD, Bruker AXS D8 Advance, Bruker, Germany), supported by the Match! program package (Crystal Impact GbR, Bonn, Germany).

The compressive strength of 3D printed scaffolds and foams was measured at room temperature using an Instron 1121 UTM (Instron Danvers, MA, USA), operating with a cross-head speed of 0.5 mm/min. Each data point represents the average value of 5-8 individual tests.

3 | RESULTS AND DISCUSSION

The effective compatibility between silicone resin/fillers mixtures and Biosilicate®, regarding the phase assemblage of the developed glass-ceramics, was verified starting from pellets obtained by uniaxial pressing. Monolithic pellets were fabricated, as reported in Table 1, using pure MK silicone with active fillers and Biosilicate glass-ceramic (in an amount varying from 0 to 70 wt.%).

Figure 2 demonstrates that the crystalline phase in samples from Biosilicate®-free formulation (100% PDC) was identical to that developed from the sinter-crystallization of Biosilicate® parent glass. More precisely, all the diffraction peaks could be ascribed to sodium-calcium silicate ($Na_2CaSi_2O_6$, ie, $Na_2O{\cdot}CaO{\cdot}2SiO_2$, PDF# 77-2189), the dominant phase in Biosilicate® glass-ceramics.[11,28] The diffraction patterns were practically coincident with each other, for the different silicone-filler/glass mixtures, in case of firing at 900°C; at 1000°C, the PDC sample exhibited much more intense diffraction peaks, which could be ascribed to enhanced crystallization degree.

The heat treatment of silicones and fillers was therefore confirmed as an effective method for the direct synthesis of glass-ceramics, as shown by previous investigations.[19,22,24] The highly reactive silica from the silicone thermo-oxidative decomposition reacted with most of the components, leading to the characteristic silicate phase, whereas P_2O_5 (from sodium phosphate) led to a liquid phase that transformed into glass upon cooling.

Interestingly, silicones and fillers were here confirmed to be not only an "alternative" technology for glass-ceramics, but also as an "integrative" technology.[19] In other words, a given glass-ceramic system could be achieved operating with only silicone and fillers (PDC approach replacing conventional glass-ceramic process) or with silicone and fillers mixed with glass powders (PDC approach integrating with the conventional glass-ceramic process). Mixtures with 30 wt% or 70 wt% glass powders, did not lead to any substantial difference in the final phase obtained after firing, except in the intensity of the peaks.

The choice of the firing temperatures was mainly based on the results from the differential thermal analysis (DTA) and thermogravimetric analysis (TG), combined with other observations on the pellets. From the TG plot of preceramic polymer and fillers (formulation G0 (100% PDC), with MK), shown in Figure 3, we can note a substantial overall weight loss. The most significant mass loss stages were detected at 510-520°C and 710-720°C, and they were attributed to the overlapping of silicone polymer-to-ceramic conversion and both Na and Ca carbonate decompositions (known to occur above 500°C[29] and above 650°C,[25] respectively). The exothermic effects of the burn-out of organic moieties probably "masked" the endothermic effect (not detected) of carbonate decomposition. The burn-out events took place up to high temperature, and they were not even complete, as the samples had a grey tint after firing. The strong exothermic peak, at approximately 900°C, could derive from the overlapping of crystallization and burn-out of residual moieties, consistent with the slight weight loss.

It is worth mentioning that different heat treatments from 900 to 1000°C were conducted to evaluate the effect of firing temperature on several parameters, such as density, shrinkage, and porosity of pellets. Table 2 reports data from different compositions after heat treatment. In general, the samples with limited Biosilicate® content (100% PDC or with 30% Biosilicate®), exhibited a substantial porosity from about 57-20 vol%. This could be an effect of the previously mentioned overlapping of burn-out of residual organic moieties and crystallization, at 900°C: gas bubbles

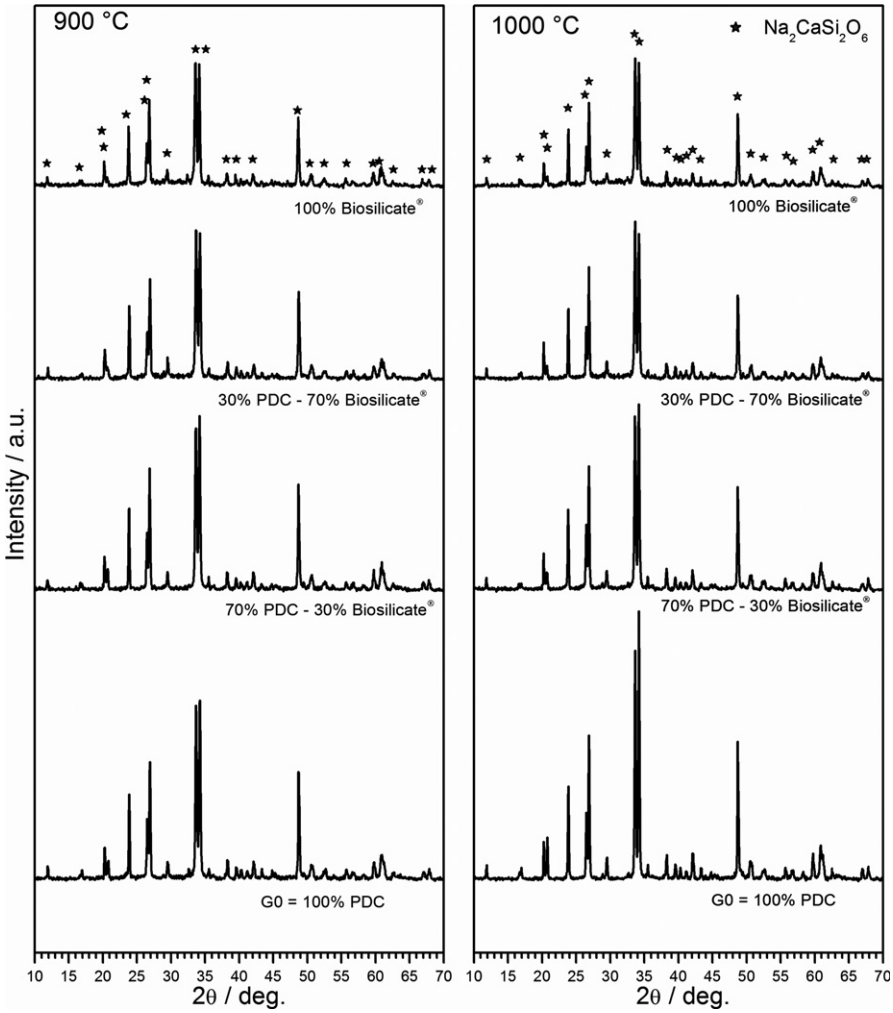

FIGURE 2 X-ray diffraction patterns of biosilicate glass–ceramics obtained from formulations G0, G30, G70, and G100 after heat treatment at 900 and 1000°C

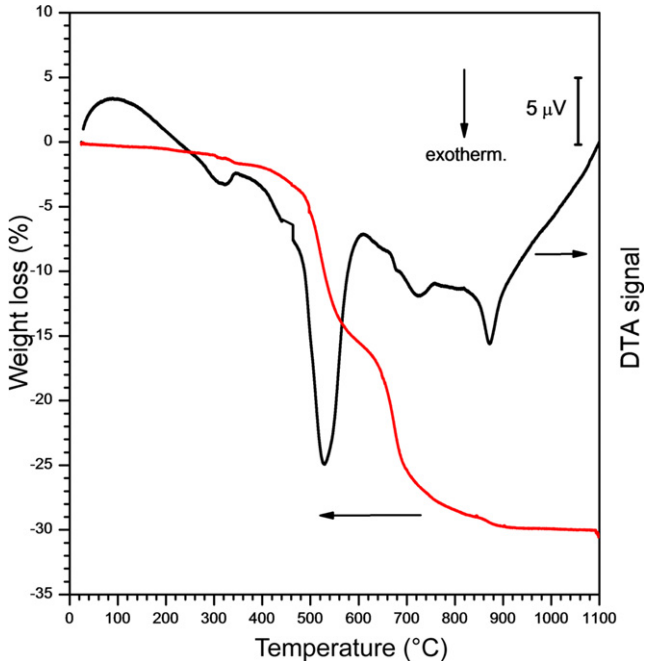

FIGURE 3 DTA and TG curves of MK silicone and active fillers (100% PDC, formulation G0) [Color figure can be viewed at wileyonlinelibrary.com]

could be somewhat "frozen" by the viscosity increase associated with the crystallization of the surrounding matrix. The significant decrease in porosity, from 900 to 1000°C, could be justified by the decreased viscosity of the residual glass phase improving sintering. Therefore, the temperature of 1000°C was employed in the further heat-treatments, based on glass-free formulations.

Figure 4 shows the morphology of reticulated scaffolds (Biosilicate®-free formulation, G0S), before and after firing. The scaffolds maintained the shape after both printing and ceramization steps. In particular, the spacing between filaments remained uniform, as visible in Figure 5A and B. The distance between filaments decreased from ~0.74 mm to 0.56 mm (see Figure 5C), whereas the filament width passed from ~0.83 mm to 0.72 mm. Figure 5D finally reveals that the filaments welded perfectly in the vertical direction: the successful interpenetration of filaments obviously favors the mechanical properties, by minimizing the stress concentrations. This is confirmed by the data reported in Table 3: with a total porosity of about 60%, the compressive strength exceeded 6 MPa, comparing well with compressive strength data (in the

TABLE 2 Density and shrinkage data concerning glass-ceramic pellets

Formulation	Temperature (°C)	Geometric density (g/cm^3)	Apparent density (g/cm^3)	Total porosity (vol%)	Radial shrinkage (%)
G0 (100% PDC)	900	1.19 ± 0.08	2.66 ± 0.03	57 ± 2	9.5
	950	1.59 ± 0.09	2.73 ± 0.04	42 ± 2	16.9
	1000	2.11 ± 0.10	2.75 ± 0.05	21 ± 2	22.2
G30	900	1.35 ± 0.05	2.69 ± 0.07	52 ± 2	9.4
	950	1.54 ± 0.06	2.82 ± 0.09	46 ± 2	12.7
	1000	2.30 ± 0.08	2.78 ± 0.03	29 ± 1	16.8
G70	900	1.80 ± 0.04	2.51 ± 0.05	32 ± 2	9.6
	950	2.11 ± 0.07	2.58 ± 0.08	31 ± 2	13.7
	1000	2.40 ± 0.03	2.61 ± 0.07	4.2 ± 0.2	14.2
G100 (100% Biosilicate®)	900	2.32 ± 0.07	2.36 ± 0.9	1.6 ± 0.1	11.1
	950	2.46 ± 0.08	2.49 ± 0.05	1.6 ± 0.1	11.2
	1000	2.53 ± 0.06	2.57 ± 0.08	1.6 ± 0.1	11.6

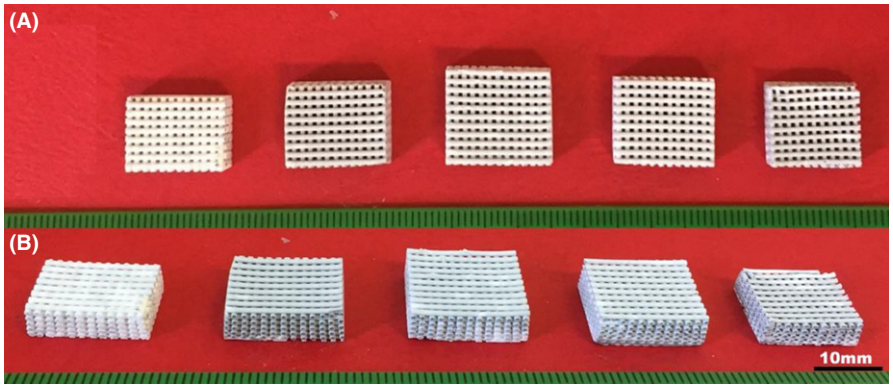

FIGURE 4 Morphology of 3D-printed scaffolds: A, green bodies after 3D printing and B, glass-ceramic samples after heat treatment at 1000°C [Color figure can be viewed at wileyonlinelibrary.com]

2-12 MPa range) of scaffolds applicable to bone regeneration.[30]

The residual porosity is attributable to the additional foaming (i.e., the formation of quite uniform pores in the cross-section, see Figure 5E and F) caused by the burn-out of moieties at high temperature. The formation of pores should not be seen as a problem, but as an opportunity for cell attachment and infiltration of body fluids; the development of hierarchical porosity (designed macro-porosity from the printing coupled with porosity in the filaments) actually represents a challenge in the manufacturing of most modern reticulated scaffolds produced by direct ink writing.[31]

The change in the formulation, with the inclusion of fumed silica, did not alter the phase formed after firing. As shown in Figure 6, sodium–calcium silicate remained the only crystal phase. As in the case of Biosilicate®-free pellets, considering the intensity of peaks, crystallization was more pronounced than that Biosilicate® glass.

As highlighted by previous investigations,[22,24] sodium phosphate is a multifunctional filler. Besides providing a liquid phase upon firing, it may cause the direct foaming of silicone-based mixtures, when used in its hydrated variant, such as $HNa_2PO_4{\cdot}7H_2O$. The dehydration reaction of this compound, as well as of similar hydrated salts (such as borax, i.e., hydrated sodium borate), determines a substantial release of water vapor, below 400°C.[19,24] The cross-linking of the polymer, at the same foaming temperature, typically stabilizes the cellular structure. The only constraint, for the adopted technique, is the use of a liquid silicone resin, to be mixed with the fillers and cast into molds just before foaming.

Figure 7 shows the effect, regarding phase evolution, of the replacement of MK, used for the fabrication of Biosilicate pellets and scaffolds, with H62C. Unlike in MK-based glass-ceramics, the crystallization occurring after firing of foamed samples at 1000°C was less substantial than that from glass-derived Biosilicate® glass-ceramics (100% Biosilicate). However, a second phase appeared, consisting of sodium calcium phosphate ($NaCaPO_4$, ie, $Na_2O{\cdot}2CaO{\cdot}P_2O_5$, PDF# 76-1456); interestingly, this is the typical phase developed when Biosilicate® parent glass, owing to a specific

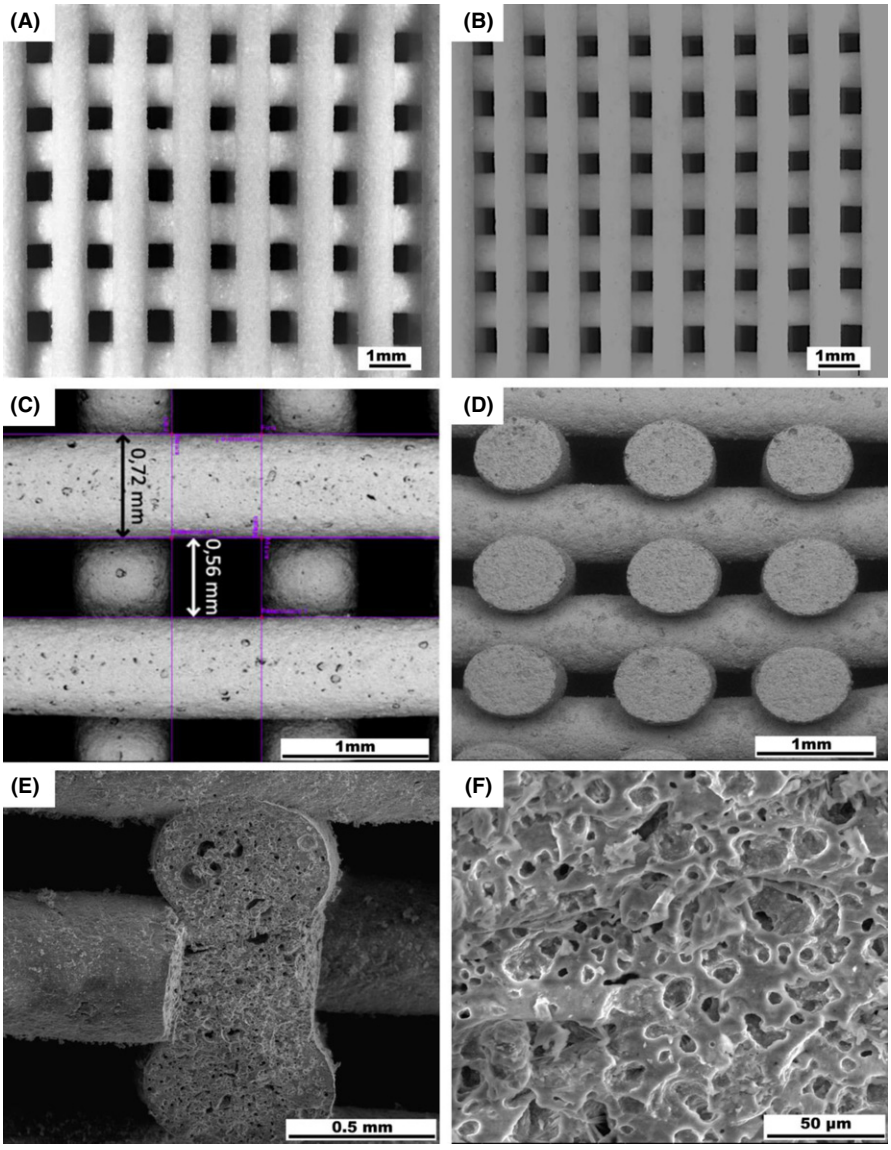

FIGURE 5 Microstructural details of 3D printed scaffolds: A, top view before firing; B, top view of ceramized scaffolds; C, detail of the spacings after ceramization; D-F, cross-section details [Color figure can be viewed at wileyonlinelibrary.com]

TABLE 3 Physical and mechanical properties of glass-ceramic foams and scaffolds produced by preceramic polymer route

Samples	Geom. density (g/cm^3)	True density (g/cm^3)	Total porosity (vol%)	Compressive strength (MPa)
G0S—3D printed scaffold	1.1 ± 0.2	2.61 ± 0.01	58	6.7 ± 0.7
G0L				
H62C-based foam	0.7 ± 0.1	2.83 ± 0.01	75	3.0 ± 0.5
G0				
MK-based foam	0.6 ± 0.2	2.70 ± 0.01	79	1.6 ± 0.4
G0B (including				
Biosilicate® powder)	0.6 ± 0.2	2.68 ± 0.01	80	5.9 ± 0.8

heat-treatment schedule, forms two crystal phases. In other words, whereas MK led to products resembling "1P" Biosilicate glass-ceramics, H62C led to a product similar to "2P" Biosilicate® glass-ceramics. This effect is probably due to different reaction paths between the silica phase, deriving from the decomposition of the preceramic polymer, and the fillers, in turn depending on the molecular architecture and composition (carbon content) of the starting preceramic polymer. The in-depth investigation of this interesting aspect is beyond the scope of this paper.

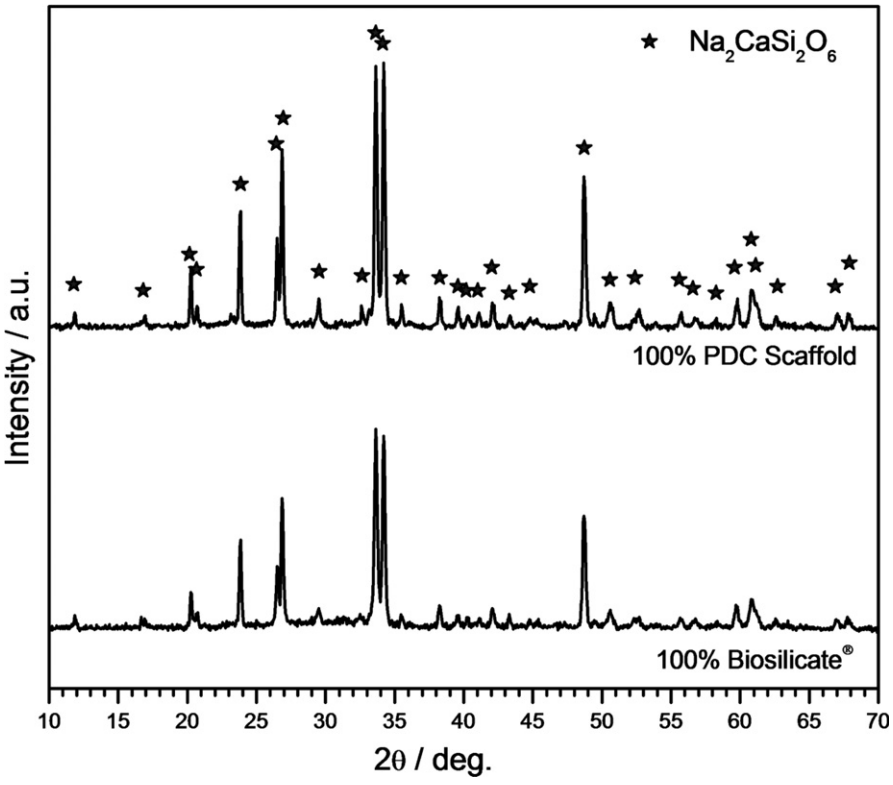

FIGURE 6 Crystallization of 3D printed scaffolds

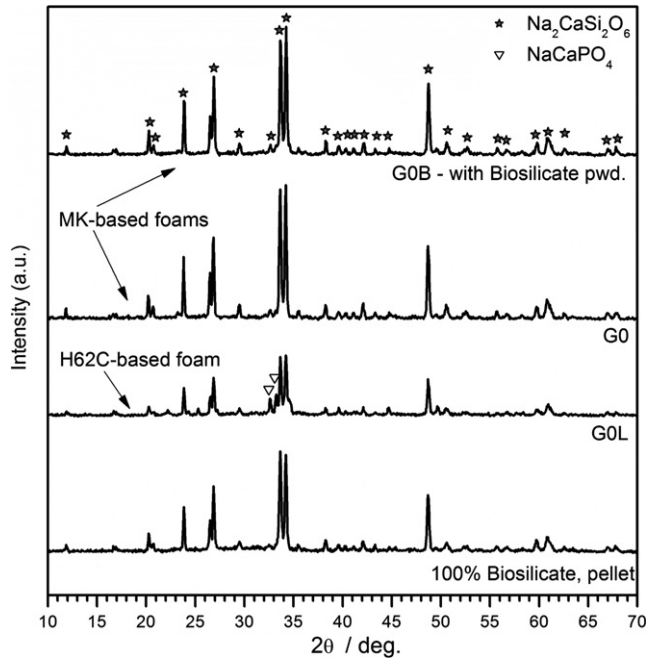

FIGURE 7 Comparison of XRD spectra of foams developed from different precursors

The behavior of MK, giving a single-crystal phase upon firing, was further confirmed also for the formulation comprising Biosilicate glass powders as additional fillers (G0B). Moreover, the use of Biosilicate glass powders aimed at improving the mechanical behavior of the produced sample (as reported in Table 3).

Figure 8 shows microstructural details of foams before and after heat treatment. For all formulations, the cellular structure developed in the polymer state was retained after firing at 1000°C. Macro-sized pores (up to 500-600 μm) were accompanied by a multitude of micro-sized pores (<10 μm). Several openings are visible between adjacent cells, mostly above 100 μm, a recognized threshold for cell ingrowth and vascularization.[32] Open porosity of the foams ranged from 73 to 79 vol%, with a limited amount of closed porosity ranged from 2 to 3 vol%.

Despite the substantial total porosity (above 75%), the glass-ceramic foams exhibited a very good compressive strength, exceeding 1.5 MPa. The best result (well above 5 MPa) was achieved by the Biosilicate® containing formulation (G0B), as a consequence, in our opinion, of a favorable overlapping of several conditions. The G0B sample, as shown in Figure 8G-L, had the most uniform microstructure both before and after firing. The reduction in the polymeric component probably enhanced the viscosity of the starting paste, in turn limiting the cell coalescence. The coarsening of cells was reduced even upon firing, owing to the remarkable crystallization, causing less residual porosity in the struts. The result may be seen as further proof of the possible integration of the conventional glass route to glass–ceramics with the new one, based on preceramic polymers and fillers.

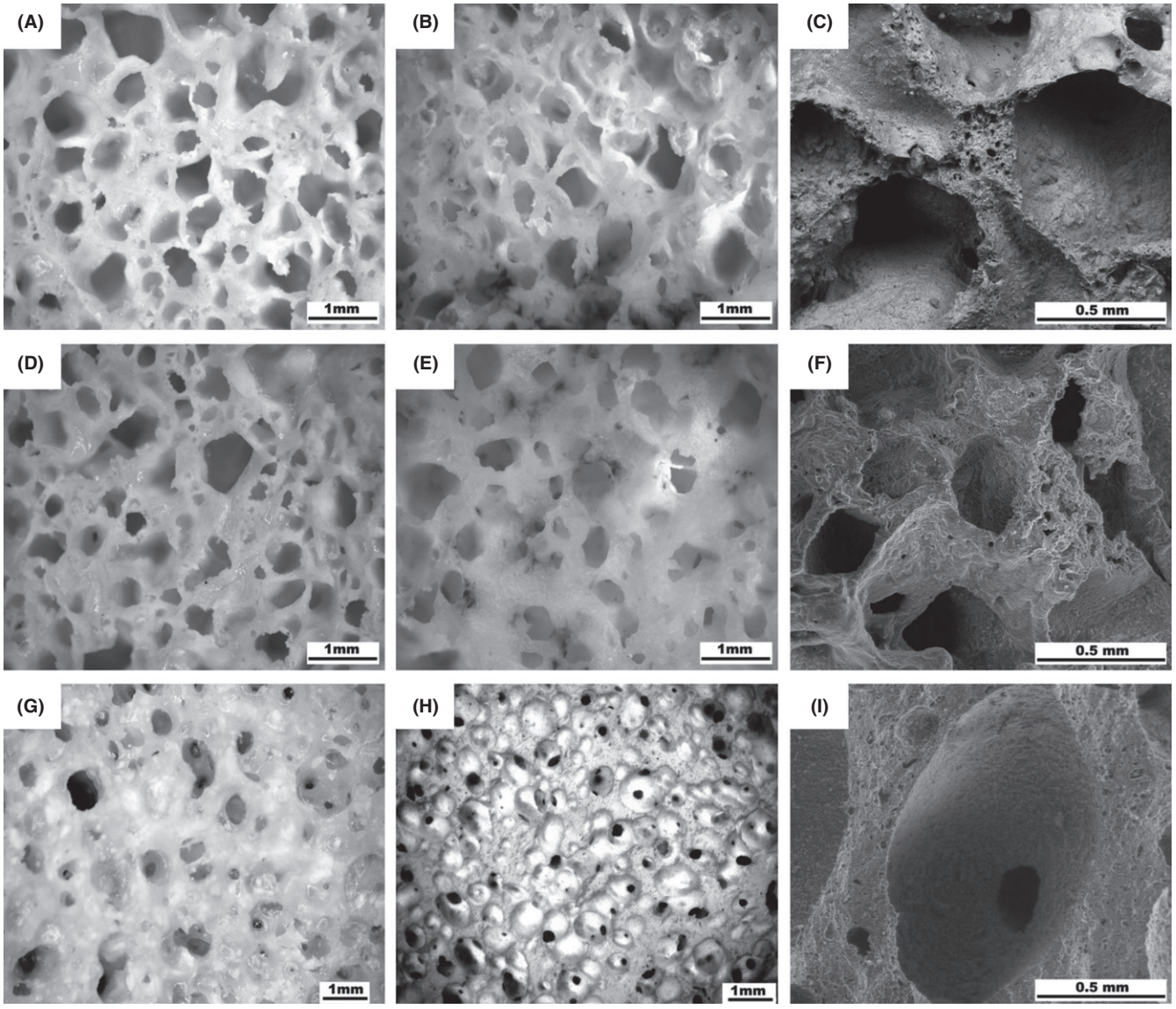

FIGURE 8 Microstructural details of polymer-derived glass-ceramic foams (A,B,C: G0L; D,E,F: G0; G,H,L: G0B) [left = before firing; centre = after firing; right = high magnification detail]

4 | CONCLUSIONS

In this work, we demonstrated that preceramic polymers containing suitable oxide precursor fillers could be employed for the direct synthesis of Biosilicate glass-ceramic in a fast and simple route, with nearly identical crystalline phases; furthermore, the present phases (one or two) can be tuned depending on the silicone polymer chosen.

The MK polymer, combined with fillers, was used for first time to produce Biosilicate scaffolds by direct ink writing; these scaffolds were composed of 720 μm thick cylindrical filaments, with a filament distance of approximately 560 μm. Despite the high porosity (approximately 60%), the Biosilicate scaffolds showed an average compressive strength of 6.7 MPa, which is superior to those of many glass and glass-ceramic scaffolds reported in the literature. Both MK and H62C polymers were also used to produce highly porous glass-ceramic foams by exploiting the water release upon dehydration, occurring at low temperature, of a phosphate filler. The Biosilicate foams exhibited high porosity (>75%) and average compressive strength in the 1.5-6 MPa range.

ACKNOWLEDGMENTS

The authors thank Dr. Laura Fiocco (University of Padova) for experimental assistance in preparing H62C-based glass-ceramic foams. Generous funding by the São Paulo Research Foundation—Fapesp CEPID grant number 2013/0079 is greatly appreciated.

ORCID

Paolo Colombo http://orcid.org/0000-0001-8005-6618
Enrico Bernardo http://orcid.org/0000-0003-4934-4405

REFERENCES

1. Kaur G, Waldrop SG, Kumar V, Pandey OP, Sriranganathan N. An introduction and history of the bioactive glasses. In: Marchi J, editor. *Biocompatible glasses. Advanced structured materials*. Cham, Germany: Springer, 2016; 53; p. 19–47.
2. Hench LL. The story of bioglass. J Mater Sci Mater Med. 2006;17:967–78.
3. Hench LL, Splinter RJ, Allen WC, Greenlee TK. Bonding mechanisms at the interface of ceramic prosthetic materials. J Biomed Mater Res Symp. 1971;334:117–41.
4. Jones JR. Review of bioactive glass: from Hench to hybrids. Acta Biomat. 2013;9:4457–86.
5. LeGeros RZ. Properties of osteoconductive biomaterials: calcium phosphates. Clin Orthop Relat Res. 2002;395:81–98.
6. Kokubo T, Kushitani H, Sakka S, Kitsugi T, Yamamuro T. Solutions able to reproduce in vivo surface-structure changes in bioactive glass-ceramic A-W. J Biomed Mater Res. 1990;24:721–34.
7. Julian RJ. Review of bioactive glass: from Hench to hybrids. Acta Biomat. 2013;9:4457–86.
8. Hench LL. Bioceramics: from concept to clinic. J Am Ceram Soc. 1990;74:1487–510.
9. Li P, Yang Q, Zhang F, Kokubo T. The effect of residual glassy phase in a bioactive glass-ceramic on the formation of its surface apatite layer in vitro. J Mater Sci Mater Med. 1992;3:452–6.
10. Peitl O, LaTorre GP, Hench LL. Effect of crystallization on apatite-layer formation of bioactive glass 45S5. J Biomed Mater Res. 1996;30:509–14.
11. Peitl O, Zanotto ED, Hench LL. Highly bioactive P_2O_5–Na_2O–CaO–SiO_2 glass-ceramic. J Non-Cryst Sol. 2001;292:115–26.
12. Montazerian M, Zanotto ED. History and trends of bioactive glass-ceramics. J Biomed Mat Res A. 2016;104:1231–49.
13. Crovace MC, Souza MT, Chinaglia CR, Peitl O, Zanotto ED. Biosilicate®—A multipurpose, highly bioactive glass-ceramic. In vitro, in vivo and clinical trials.. J Non-Cryst Sol. 2016;432:90–110.
14. El-Rashidy AA, Roether JA, Harhaus L, Kneser U, Boccaccini AR. Regenerating bone with bioactive glass scaffolds: a review of in vivo studies in bone defect models. Acta Biomat. 2017;62:1–28.
15. Jones JR, Boccaccini AR. Biomedical applications: Tissue engineering. In Colombo P, Scheffler M, editors. *Cellular ceramics: Structure, manufacturing, properties and applications*. Weinheim, Germany: Wiley-VCH Verlag GmbH &Co. KGaA, 2005; p. 547–70.
16. Bernardo E, Colombo P, Dainese E, Lucchetta G, Bariani PF. Novel 3D wollastonite-based scaffolds from preceramic polymers containing micro- and nano-sized reactive particles. Adv Eng Mat. 2012;14:269–74.
17. Cacciotti I, Lombardi M, Bianco A, Ravaglioli A, Montanaro L. Sol-gel derived 45S5 bioglass: synthesis, microstructural evolution and thermal behaviour. J Mater Sci Mater Med. 2012;23:1849–66.
18. Elsayed H, Zocca A, Bernardo E, Gomes CM, Günster J, Colombo P. Development of bioactive silicate-based glass-ceramics from preceramic polymer and fillers. J Eur Ceram Soc. 2015;35:731–9.
19. Fiocco L, Elsayed H, Daguano JKMF, Soares VO, Bernardo E. Silicone resins mixed with active oxide fillers and Ca–Mg silicate glass as alternative/integrative precursors for wollastonite-diopside glass-ceramics foams. J Non-Cryst Sol. 2015;416:44–9.
20. Zocca A, Elsayed H, Bernardo E, Gomes CM, Lopez-Heredia MA, Knabe C, et al. 3D-printed silicate porous bioceramics by using a non-sacrificial preceramic polymer binder. Biofabrication. 2015;7:025008.
21. Ohl C, Kappa M, Wilker V, Scheffler F, Scheffler M. Novel open-cellular glass foams for optical applications. J Am Ceram Soc. 2011;94:436–41.
22. Elsayed H, Colombo P, Bernardo E. Direct ink writing of wollastonite-diopside glass-ceramic scaffolds from a silicone resin and engineered fillers. J Eur Ceram Soc. 2017;37:4187–95.
23. Fiocco L, Babakhanova Z, Bernardo E. Facile obtainment of luminescent glass-ceramics by direct firing of a preceramic polymer and oxide fillers. Ceram Int. 2016;42:6770–4.
24. Fiocco L, Elsayed H, Ferroni L, Gardin C, Zavan B, Bernardo E. Bioactive wollastonite-diopside foams from preceramic polymers and reactive oxide fillers. Materials. 2015;8:2480–94.
25. Zocca A, Franchin G, Elsayed H, Gioffredi E, Bernardo E, Colombo P. Direct ink writing of a preceramic polymer and fillers to produce hardystonite $Ca_2ZnSi_2O_7$ bioceramic scaffolds. J Am Ceram Soc. 2016;99:1960–7.
26. Zocca A, Colombo P, Gomes CM, Günster J. Additive manufacturing of ceramics: issues, potentialities, and opportunities. J Am Ceram Soc. 2015;98:1983–2001.
27. ASTM International. Standard Test method for water absorption, bulk density, apparent porosity and apparent specific gravity of fired whiteware products. Designation: 2006; C 373-88.
28. Hench LL, Polak JM. Third-generation biomedical materials. Science. 2002;295:1014–7.
29. Fang H-X, Li H-Y, Xie B. Effective chromium extraction from chromium-containing vanadium slag by sodium roasting and water leaching. ISIJ Int. 2012;52:1958–65.
30. Rahaman MN, Liu X, Huang TS. Bioactive glass scaffolds for the repair of load-bearing bones. In R N, P C, editors. *Advances in bioceramics and porous ceramics*. Hoboken, NJ: John Wiley & Sons, 2009; 32; p. 65–78.
31. Machado GC, García-Tuñón E, Bell RV, Alini M, Saiz E, Peroglio M. Calcium phosphate substrates with emulsion-derived roughness: processing, characterisation and interaction with human mesenchymal stem cells. J Eur Ceram Soc. 2018;38:949–61.
32. Rahaman MN, Day DE, Bal BS, Fu Q, Jung SB, Bonewald LF, et al. Bioactive glass in tissue engineering. Acta Biomat. 2017;7:2355–73.

How to cite this article: Elsayed H, Rebesan P, Crovace MC, Zanotto ED, Colombo P, Bernardo E. Biosilicate® scaffolds produced by 3D-printing and direct foaming using preceramic polymers. *J Am Ceram Soc*. 2019;102:1010–1020. https://doi.org/10.1111/jace.15948